

# **STAR Heavy Flavor Tracker (HFT)**

## **Response to CD-0 Questions**

**Version 3 April-28 : 18:00**

**April 28, 2009**

## 1. Introduction

This report is written in response to the questions raised in the report Scientific Review of the Proposal “A Heavy Flavor Tracker for STAR”. In the first part we describe in detail the simulations that have been performed since the submission of the proposal and address all the relevant questions. In the second part we perform a first risk analysis of the six specific points laid out in the report from DOE.

In the Appendix we list the relevant excerpts from the DOE report that we have attempted to answer in this report.

## 2. HFT Simulations

In this section we address the simulation part of the report, namely to:

- Repeat full/refined physics-performance simulations with the proposed configuration of detectors.
- Quantitative evaluations of impact of a variety of effects (e.g. TPC space charge, realistic PID, detector thickness etc) on overall detector performance and physics observables. This analysis should also include a scenario where either the SSD or IST layer suffers a catastrophic failure as a whole.



### 2.1. Simulation Environment

In this report all simulations were done using the standard STAR software chain, i.e. the same environment that is used to perform acceptance and efficiency studies and corrections to our data (via embedding). The HFT detector configuration (geometry) is a representative but simplified version of the proposed apparatus, i.e. all detectors are represented at the correct radius and with our current best estimate of average radiation thickness. At this point no complex support structures are included as discrete components in the simulation, just their average radiation thickness, one of the reasons being that they were still not known at the time the geometry was defined. The complete HFT geometry comprises of two layers of PIXEL detectors at 2.5 and 8 cm radius, one IST layer of 600 (r- $\phi$ ) x 6000 (z) micron strip-lets at a radius of 14 cm and the existing SSD detector at 23 cm radius.

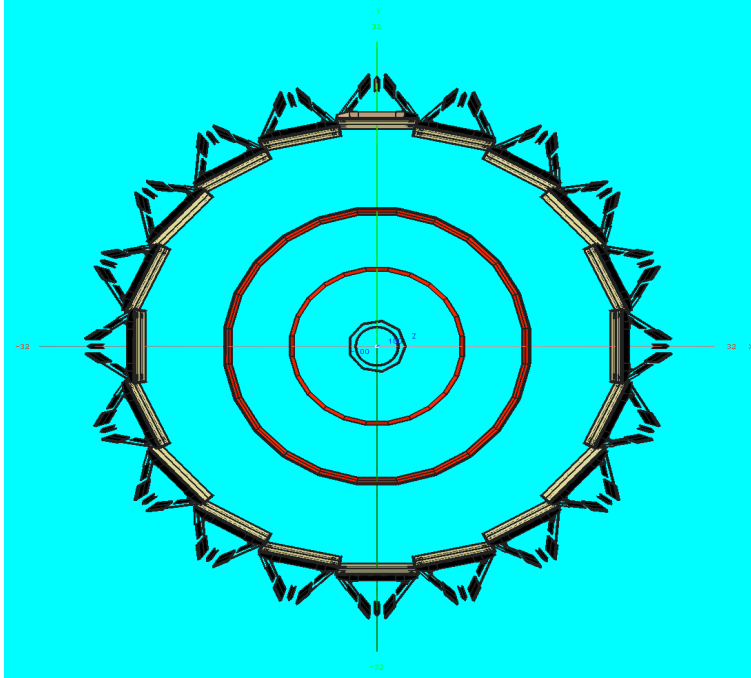


Figure 1: A schematic cross section of the HFT detector in STAR simulation environment

A sketch of HFT is shown in fig. 1. In the **standard HFT** configuration the beam pipe has the final thickness of 0.75 mm instead of 0.5 mm. The PIXEL layers have a total thickness of  $0.32\% X_0$  per layer and the IST of  $1.32\% X_0$ . In order to estimate the sensitivity of the system to mass thickness we also ran simulations with varying IST thicknesses and the PIXEL layer increased to  $.62\% X_0$  per layer to simulate, even though slightly overestimated, the possible use of Cu instead of Al traces on the readout cables. Full simulations were also run for the hypothetical case of a catastrophic failure of either the SSD or IST and the impact of such scenario to physics was estimated. The **detector response** simulators that we used in the simulations represent our best estimates of the detector performance. For the SSD (which is a detector already in use in STAR) we used the standard simulator w/out dead modules (since the detector have been serviced and repaired for HFT). For IST we used a standard (for strip detectors) hit smearing appropriate for the give pad size and w/out dead areas. For the PIXEL layers a 9 microns hit smearing was included, as the current best estimate of the anticipated position resolution.

The **standard tracking** software was used for tracking with only minor ‘search area’ optimized parameters. This is an area where further tuning and improvements are possible and very promising, e.g. the use of standard techniques like momentum ordering and/or event vertex constraint, but we find the tracking performance adequate for this study.

A new, more **realistic PID** method deployed by STAR was used in these simulations with the inclusion of the full TOF barrel in the simulations and the analysis.

The **simulation data sample** consists of about 10 K *Hijing* events embedded with 5  $D^0$ /event. All  $D^0$  were forced to decay 100% in the K-pi channel for useful signal statistics but all physics performance figures are scaled to the expected charm cross



sections. The size of this sample is comparable to the one used for the CD0 review and the HFT proposal studies.

All other conditions are identical to CD0-review ones, e.g. beam luminosity, pile-up densities in the PIXEL layers etc.

## 3. Results

### 3.1. Full System D-meson Physics Performance

The obtained results are presented below. We first start with the **standard HFT** refined simulation results and we will compare them to those presented during the CD0 review. Figure 2 shows the resulting  $D^0$  reconstruction efficiency. The red points show the reconstructable fraction of the decays, before any optimization cuts are applied; it is therefore an upper limit. If the two decay tracks are successfully reconstructed in the TPC and with, at least, the two Pixel hits correctly assigned to the track, then the decay is characterized as reconstructable. This fraction starts at about 20% at low  $p_T$  and slowly rises to about 30% at high  $p_T$ . The black points show the fraction of decays that pass the reconstruction cuts and they strongly depend of the particular choice of cut values. For this study we used the **same** set of cuts as for the CD0 review analysis in order to make apple-to-apple comparisons. These cuts explore the topological/geometrical features of real decays and are the indispensable tool that suppresses the background by several orders of magnitude, to levels that an acceptable S/N ratio is achieved. More details on the used cuts can be found in the HFT proposal.



We observe that the new (open) points do not show any significant difference from what was presented at the CD0 review for both the red and the black points. This is a coincidence due to cross cancelling of various effects. The thicker beam pipe and the detailed, more realistic TOF-PID included here should have somewhat reduced the “new” efficiency but a slight optimization of the search tracking parameters seems to have compensated for the loss. The striking similarity of the efficiencies signals no major surprises in the physics performance with the new simulations provided that the background levels remained also similar. This latter point is addressed in detail in the following paragraphs.

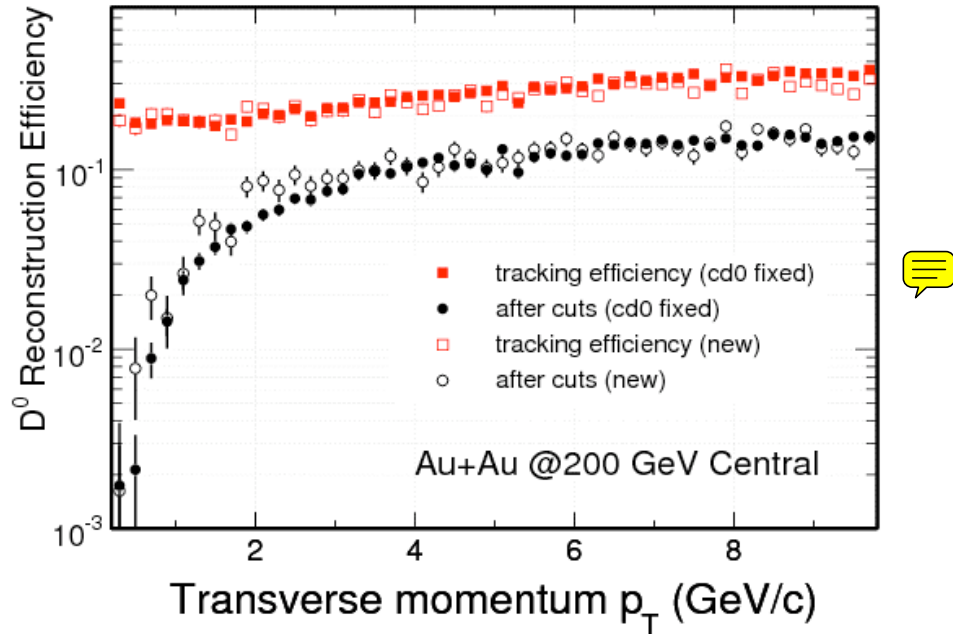


Figure 2: (Red line) Fraction of reconstructable  $D^0$  mesons. (Black line) Fraction after a certain set of cuts has been applied to suppress background. Filled symbols are the CD0 review points and Open ones are this simulation.

The next step in the analysis, in order to estimate the physics performance, is a careful evaluation of the S/B as a function of  $p_T$  which should, among other things, include: a) a proper signal rescaling so that the number of embedded  $D^0$  reflects the anticipated charm production cross section, and b) the careful evaluation and rescaling of background levels including those resulting from combining a  $D^0$ -daughter track with a random track from the event. As STAR and PHENIX differ in their estimates of total charm production cross section by about a factor of two, we used the lower of the two estimates (PHENIX). Figure 3 shows the resulting signal significance levels and its error for an extrapolated 500 millions event sample. The size of this data sample is expected to reflect 2-3 months of RHIC running time, if one uses realistic duty factors (20-40%) in data taking. We see that excellent levels can be achieved even at low  $p_T$  values. We can now use this information and fold it with an **expected  $p_T$  shape** in order to simulate a resulting  $p_T$  distribution. Figure 4 shows how the anticipated D-meson  $p_T$  spectrum for the same extrapolated sample is going to look like. Notice the broad range of  $p_T$  reach and the expected accuracy of the points. This sample is expected to be the result of a year's run (~6 months of RHIC running). We observe that we can achieve good signal significance for a wide range of transverse momentum values, starting almost at zero  $p_T$  (a realistic cut off value for an acceptable S/N ratio is around 300 MeV/c).

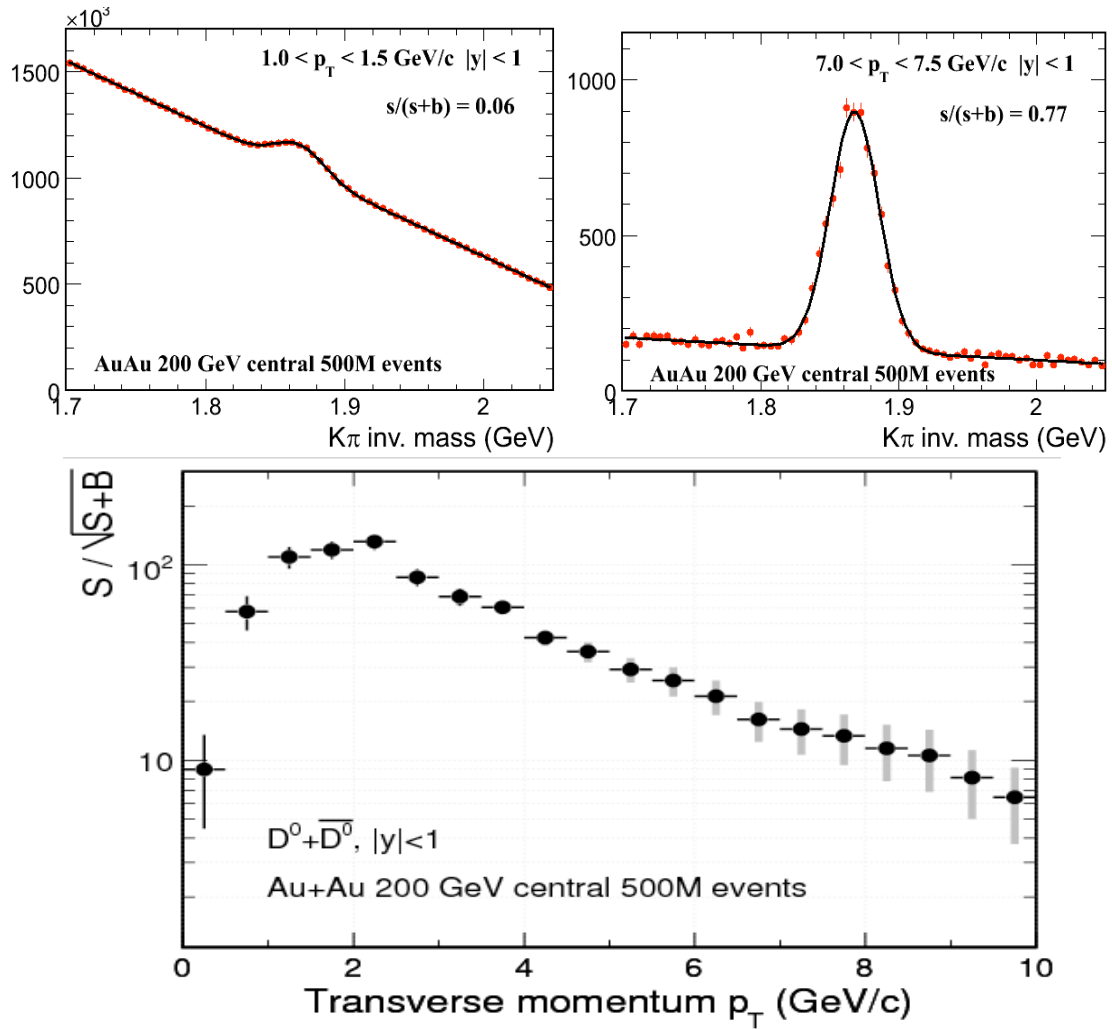


Figure 3 Invariant Mass distributions (upper panels) for both very low and high  $p_T$  bins. Signal significance levels (and estimated error) as a function of  $p_T$  extrapolated to 500 million events

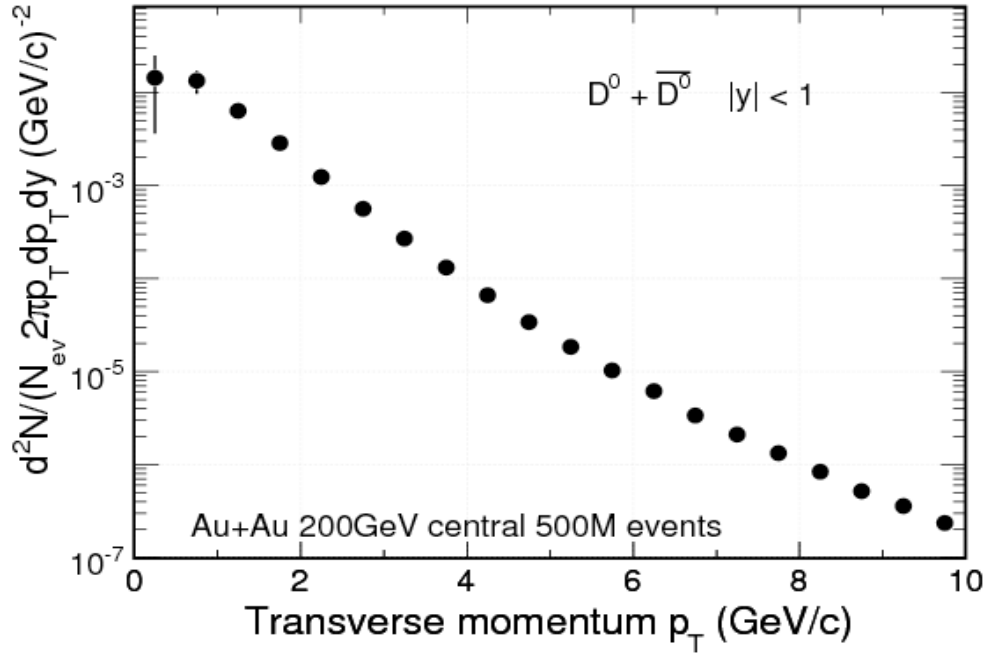


Figure 4: Estimated D-meson  $p_T$  distributions

The next two figures (Figure 5 and 6) show the updated resolution for the two key measurements of HFT, the elliptical flow parameter  $v_2$  (fig. 5) and the flavor suppression factor  $R_{CP}$  (fig. 6). The error bars are estimated using the results of the new simulation. If we compare fig.5 with the one in the HFT proposal we will see that our new, more refined analysis leads to slightly smaller errors at low transverse momenta (mainly due to a better PID analysis module) and an increase (by almost a factor of two) of the errors at the largest  $p_T$  values (mainly due to better background evaluation).

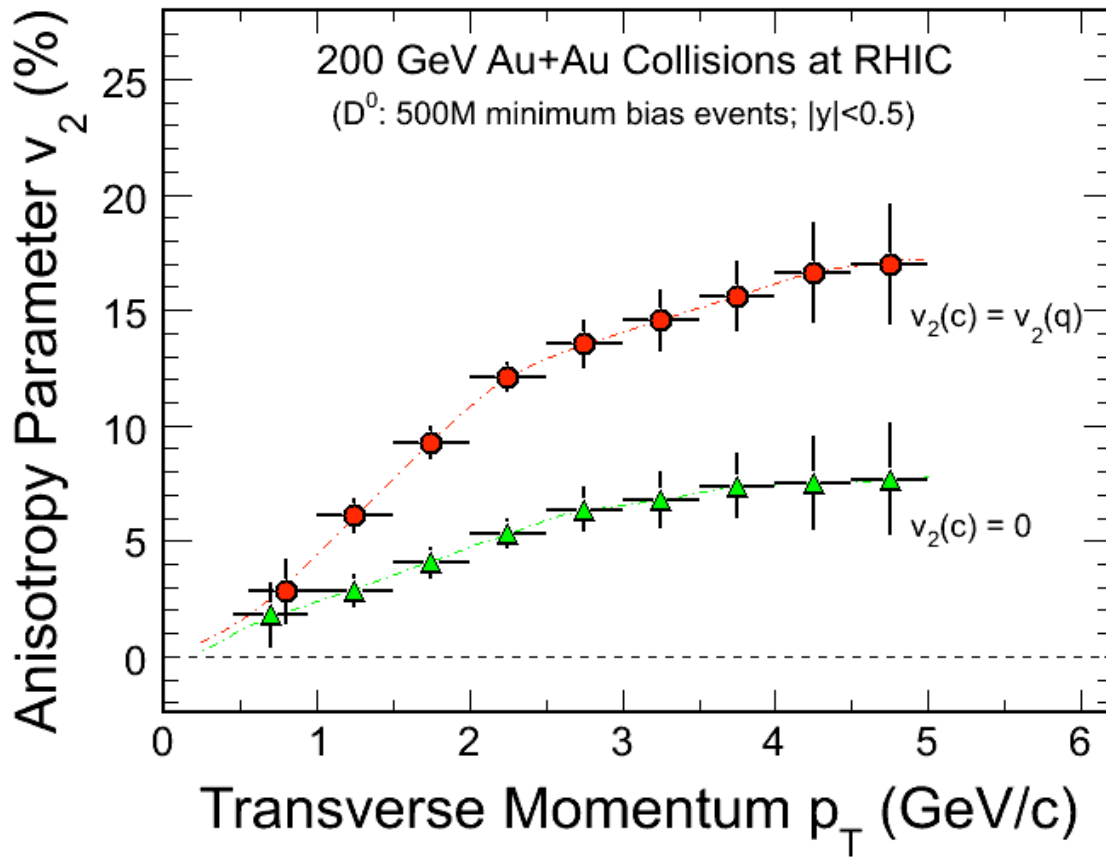


Figure 5: Charm elliptic flow with HFT for two extreme case scenarios

The new fig. 6 compared to the one in the proposal shows similar features at the extreme values of transverse momenta (??).



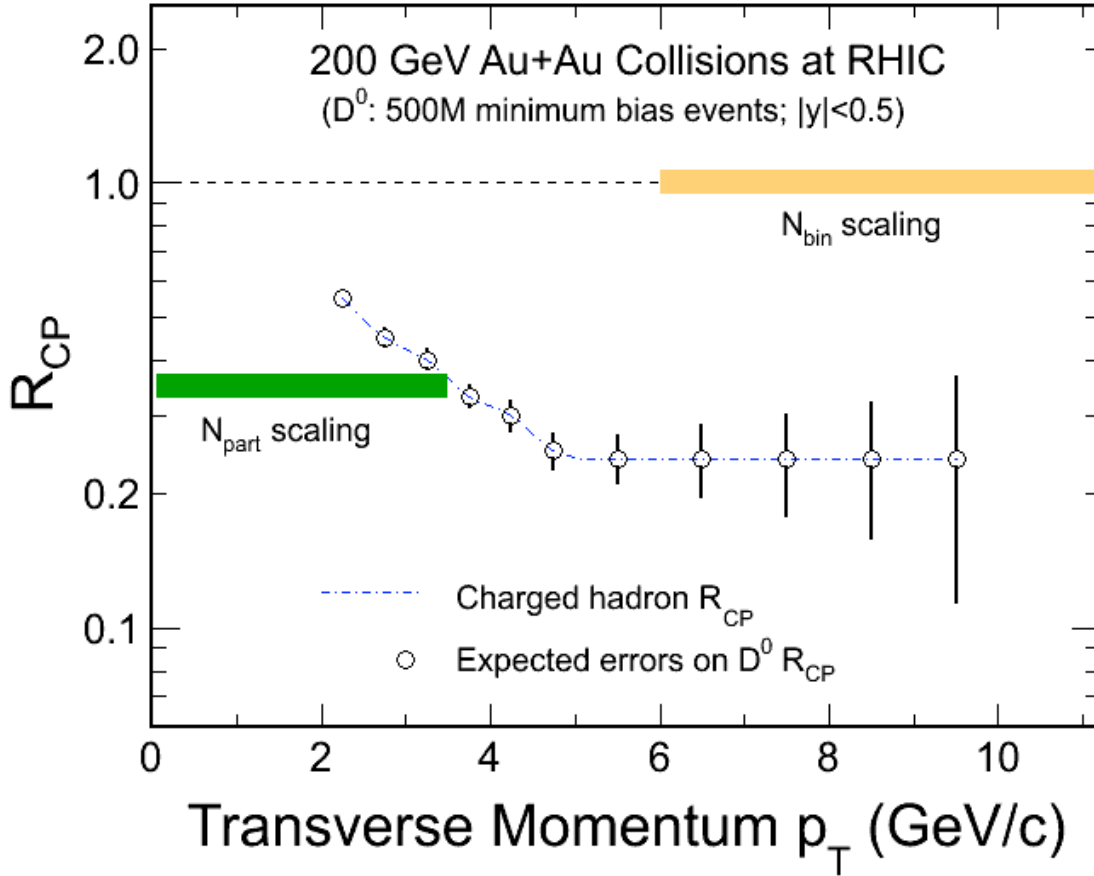


Figure 6: Direct Charm  $R_{CP}$  determination (and related uncertainties) with HFT



### 3.2.Failure Analysis – System performance without SSD or IST

We performed simulations where either the entire SSD or the IST layers were effectively not functional, i.e. their hit information was not available to the tracking packages. The impact on physics observables of this hypothetical scenario comes exclusively through its modification of the overall system tracking efficiency, since the pointing accuracy of HFT is primarily determined by the PIXEL layers. The results are shown in fig. 7 (full simulation) and fig. 8 (Fast-MC) as the single track reconstruction efficiency for pions. The black points (line) shows the efficiency of the full system, the blue points (line) the efficiency in the case of dead-IST and the red points (line) the efficiency for dead-SSD. The absolute scale of the Fast-MC is 5-8% higher than the full simulation but this is expected since the Fast-MC is a more idealized environment. As we analyze the results we should keep in mind that one of the design goals of HFT was to have built-in redundancy in tracking just for this case, i.e. the failure of a critical, intermediate tracking layer. Both simulations are in good agreement for the no-SSD case, showing an average loss of efficiency of about 5-8% depending on  $p_T$ . For the no-IST case the Fast-MC shows a much smaller efficiency loss than the full simulation. We understand this to be the result of a more realistic SSD geometry (with dead areas in the periphery of the wafer, i.e. lower geometrical ‘efficiency’) in the full simulations as opposed to a hermetic

coverage in Fast-MC. This difference does not exist in the case of no-SSD since both geometries have complete coverage. By squaring the absolute single track efficiency in the various cases, as obtained by the full simulations, we can estimate the expected loss of  $D^0$  efficiency, which comes out to be about 5% on the average absolute efficiency loss or about 20% relative loss (from  $\sim 25\%$  to  $\sim 20\%$ ). A similar relative loss is predicted by the Fast-MC (dashed lines).

On top of this efficiency loss we also expect a slight increase of the background levels, since any single track inefficiency results in an increased rate of ghost tracks. This level is expected to be minimal after the selection software cuts are applied. Full simulation studies showed that the level of ghost tracks (before cuts) increases by 0-10%, depending on  $p_T$  therefore the impact on the S/N is expected to be minimal. We conclude that the loss of an entire layer of the intermediate tracking system has a sizeable impact on the system performance but, until repairs are done, the key physics measurements would be successfully carried on. As a final note on this subject let us remember that this failure analysis used the tracking software w/out any modifications. In real-life, tracking optimization techniques will be deployed in order to clean up and recover part of the lost efficiency; therefore what is presented here is a rather extreme, pessimistic scenario.

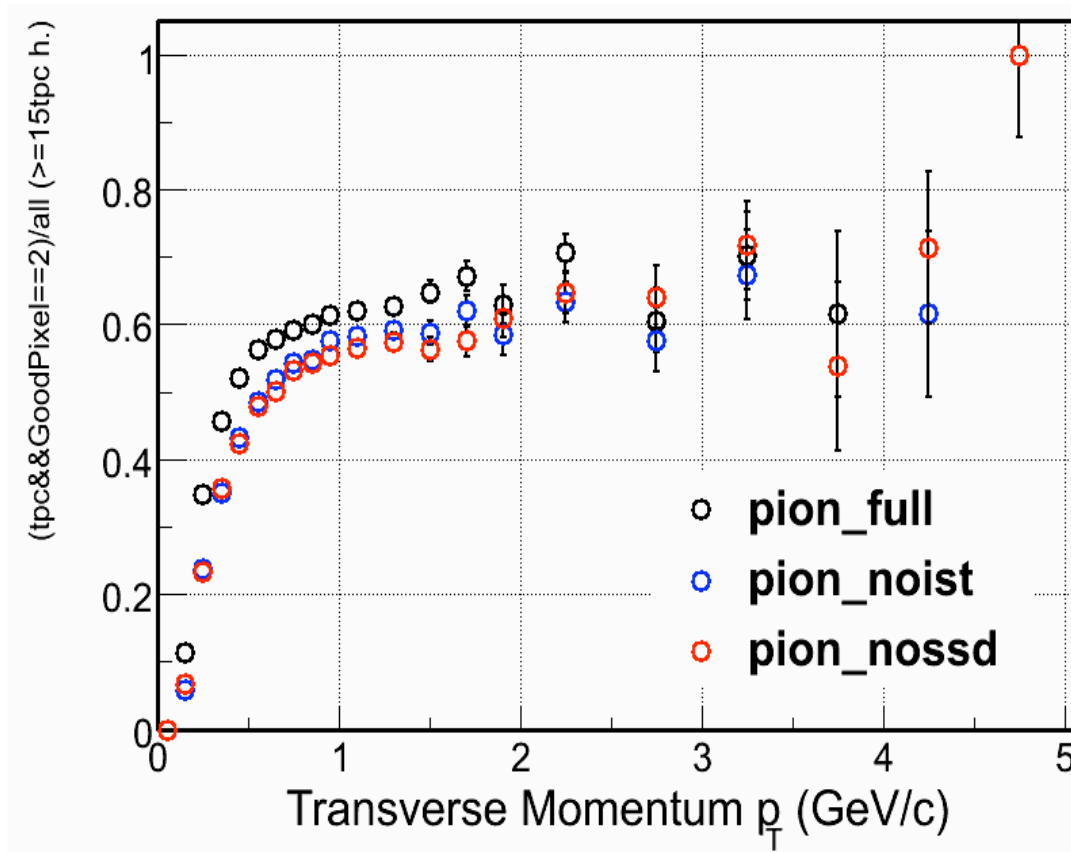


Figure 7: Single track reconstruction efficiency for the case of a FULL HFT (black), dead IST (blue) and dead SSD (red) points

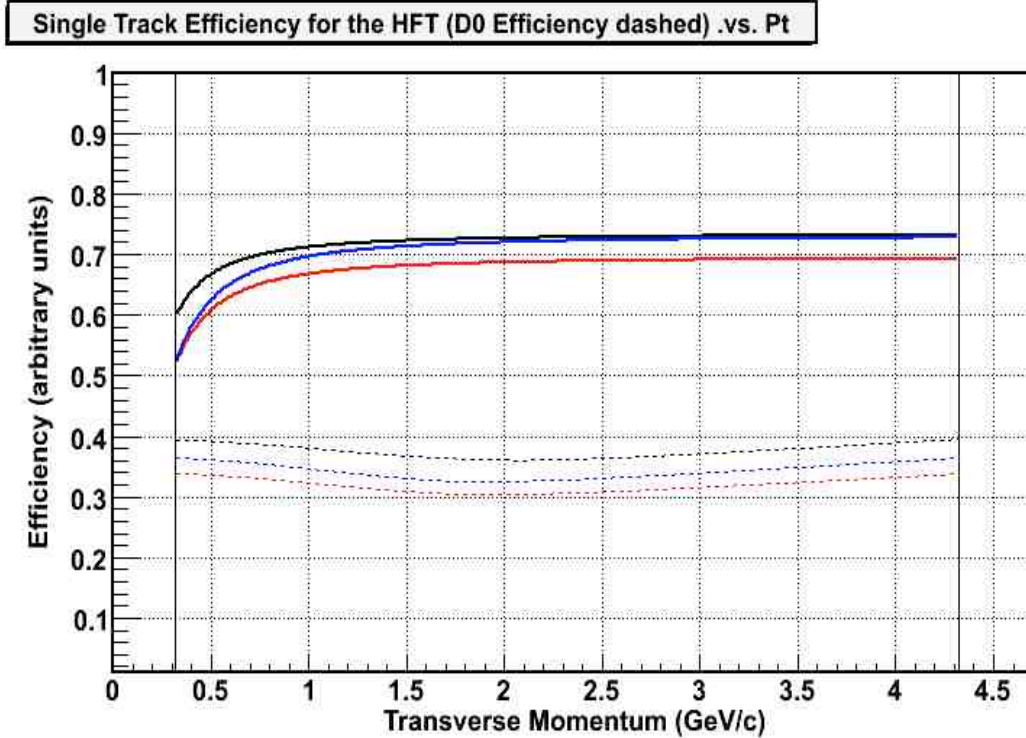


Figure 8: Same as fig. 7 but from Fast-MC. The dashed lines show the impact on  $D^0$  efficiency before cuts.

### 3.3. Full System Performance for various Thickness Scenarios

One of the committee’s concerns was whether the PIXEL and IST material budget was realistic so it asked for a system performance study as a function of thickness. The main items of concern are the prospect of water-cooling of the IST electronics and the PIXEL readout cables and support (e.g. vibrational/cooling stability). A lot of work has been done since the review to experimentally assess the proposed PIXEL support stability for air-cooling and thermal expansions and the results verified the expected/anticipated behavior within the design parameters. The only remaining issue is the possible use of Cu instead of Al traces on the PIXEL readout cables. The use of copper will increase the total material budget in the PIXEL from about 0.3% to 0.52%  $X_0$ , but in our simulations we opted (for convenience) for an even more pessimistic value of 0.62%. For the IST, the inclusion of a possible water-cooling system in the simulations was done the same way, i.e. by effectively doubling its overall radiation thickness. The impact of radiation thickness of the IST is different than that of the PIXEL detector. In the former case only the  $D^0$  signal is affected through the modification of the single track efficiency whereas in the latter case the impact primarily comes from the degradation of the pointing resolution (DCA) due (mainly) to a thicker first PIXEL layer. This DCA degradation impacts both signal recovery, after the selection cuts have been applied, and background levels.

For the thick-IST case (i.e. 2x thick) fig. 9 (Full and Fast-MC) both agree that the impact is less than 5%, which has minimum impact on physics.

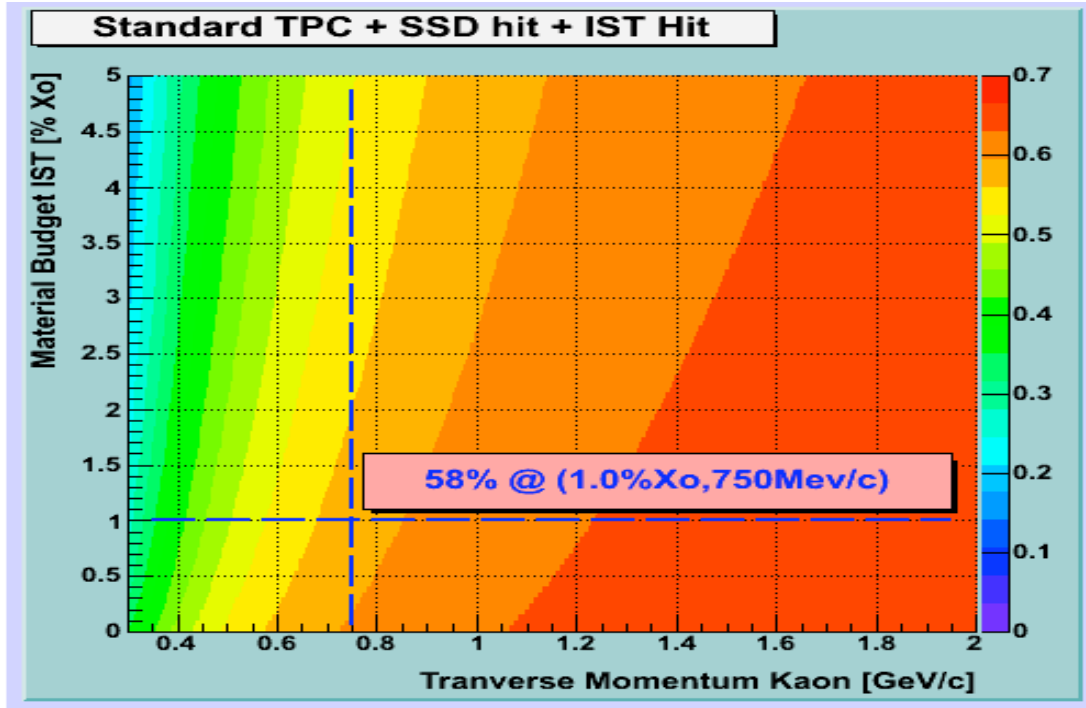


Figure 9: Fast-MC calculations for single track efficiency as a function of  $p_T$  and IST thickness.



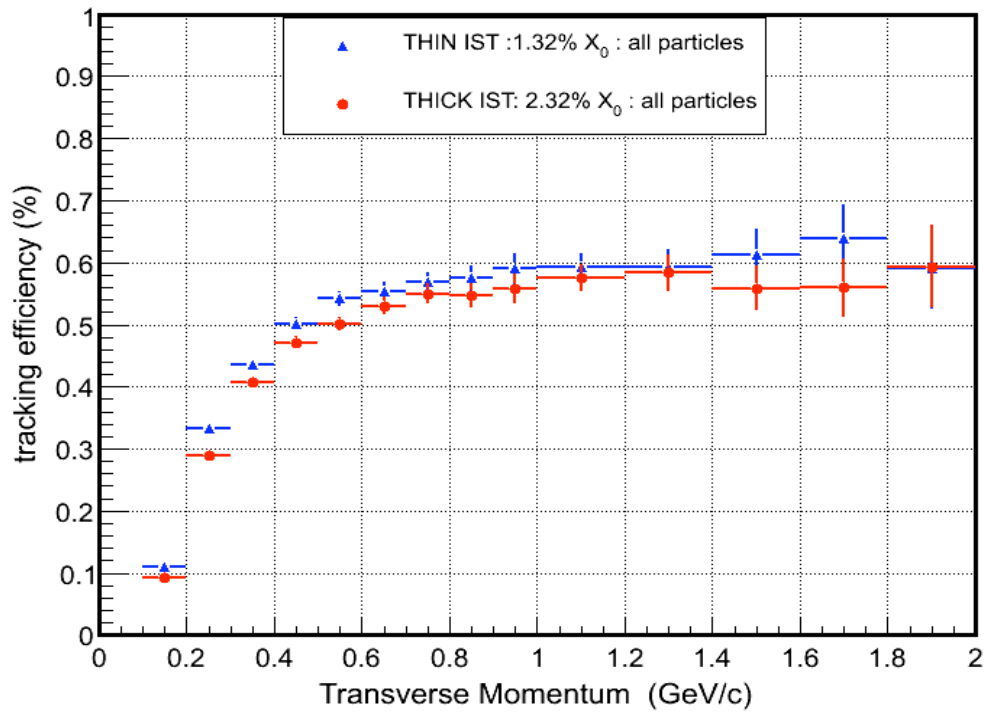


Figure 10: The impact of a doubly thick IST (red points) on single tracking efficiency. The blue points are for the standard IST case.

The case of a thicker PIXEL detector is more complex. The thickness impact on single-track (and D0) efficiency is expected to be minimal. This is shown in fig. 10 that shows that the single-track efficiency effect is about 1% and the effect on D0 efficiency about 2%.



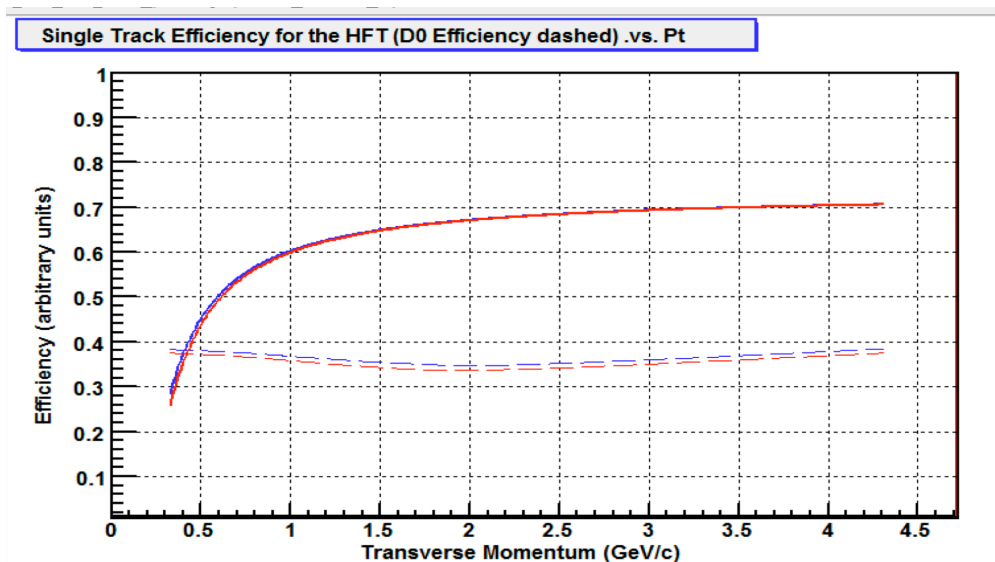


Figure 11. Impact of thicker PIXEL on single track (solid) and D0 (dashed) efficiency before cuts. The standard PIXEL is in blue and the thicker one in red.

The impact of a thicker PIXEL layer on DCA we can see in fig. 12 that shows the transverse-plane impact parameter (DCA) resolution as a function of  $p_T$  for both full (upper panel) and Fast-MC (lower panel) simulations. We see that for  $p_T=1$  GeV/c the DCA increases by about 8 microns (from 22 to 30). This, in turn, affects both the signal efficiency after the cuts are applied and the expected background levels, therefore the accuracy of the physics observables for a given number of events. In order to estimate this we ran a full-scale simulation with the thicker PIXEL since the Fast-MC cannot answer this question. Figure 12 show the effect of the thicker PIXEL on D0 efficiency before and after the cuts compared to the standard and CD0 cases. We see that the impact is finite but limited. The impact is more pronounced in the background levels. The full discussion of the results is done in section 4.2 below.

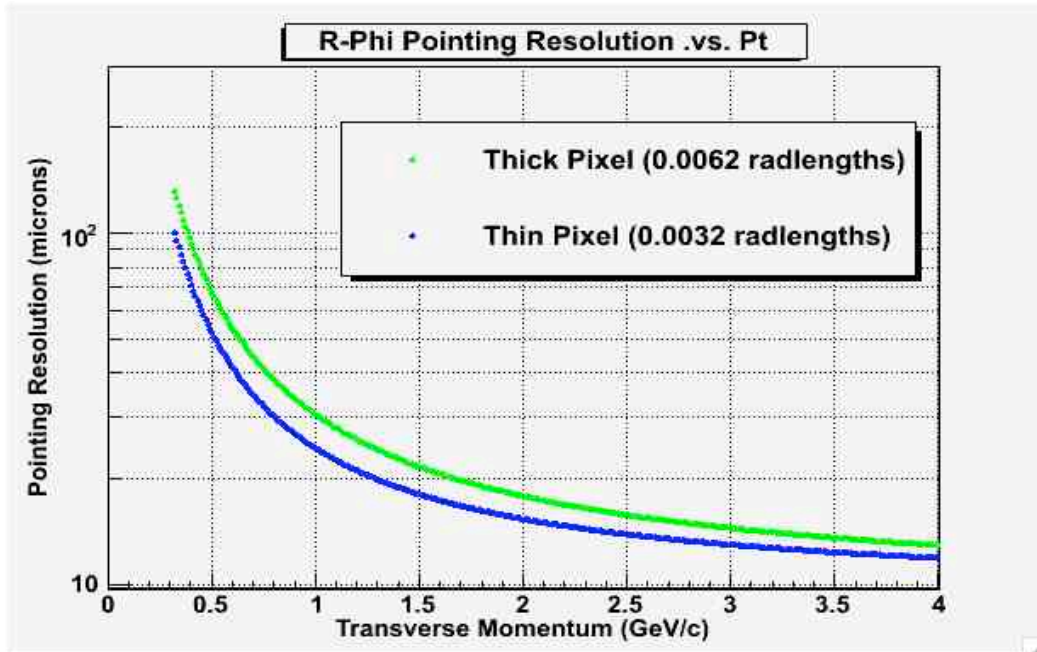
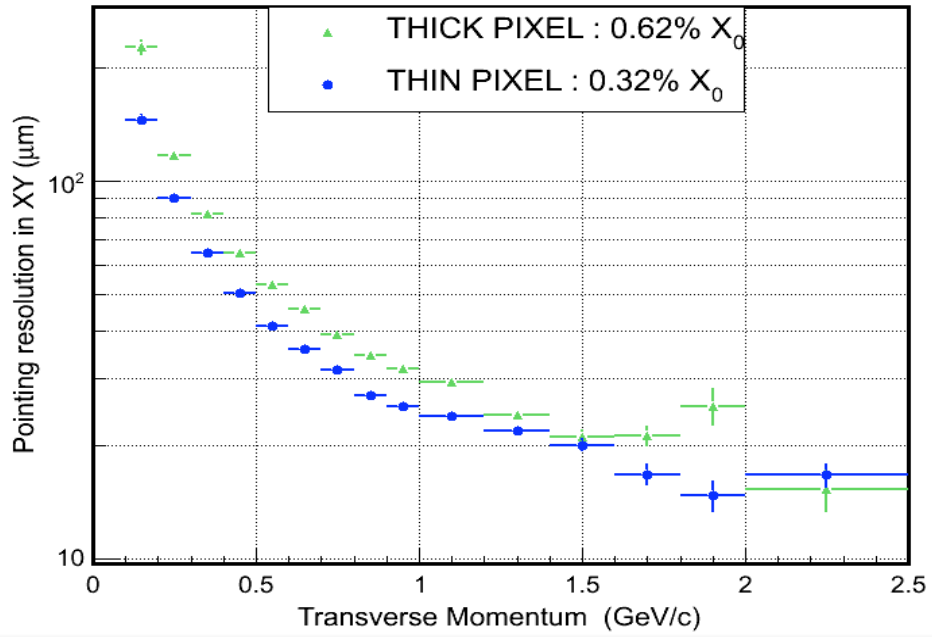


Figure 13: Impact of a thicker PIXEL detector on DCA resolution for Full (upper) and Fast (lower) simulations

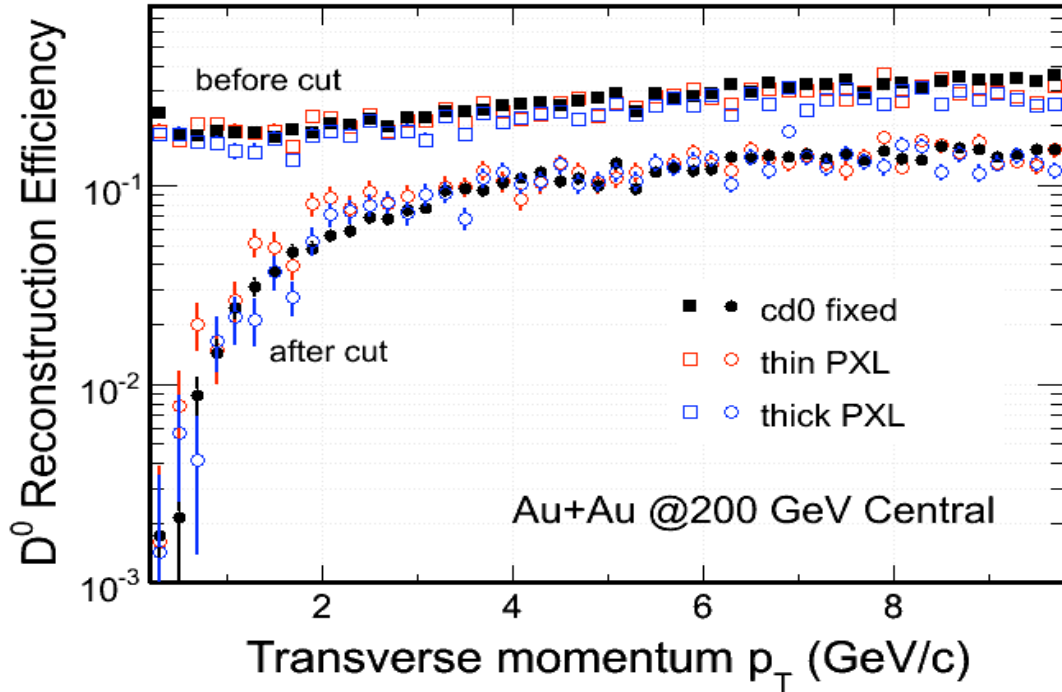


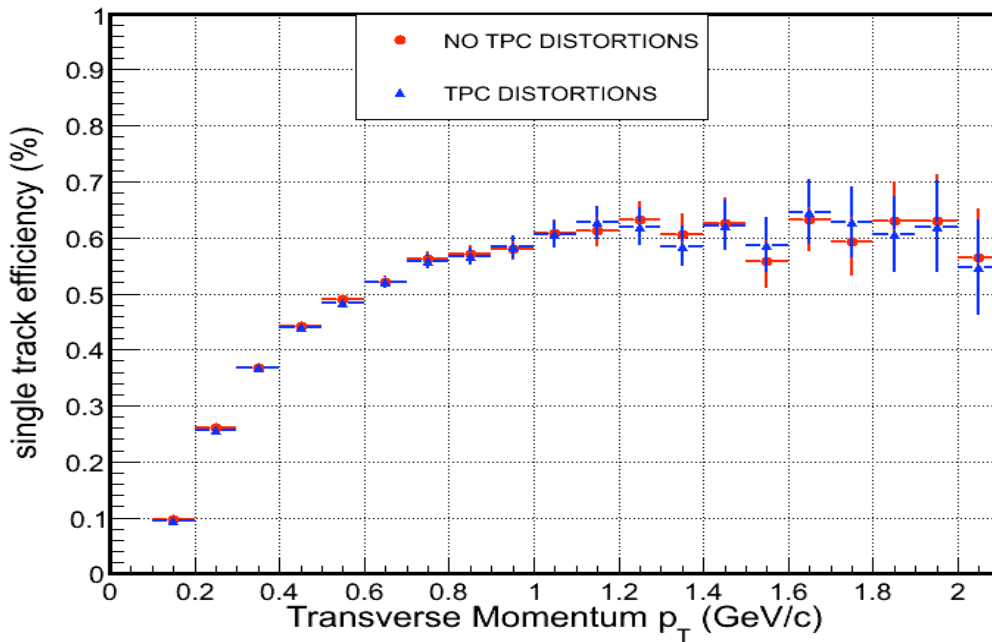
Figure 14: Effect of the thicker PIXEL on  $D^0$  efficiency before and after the cuts compared to other cases.

### 3.4. Effect of increased TPC Space Charge

We have also studied the effect of increased space charge (distortions) in the TPC are going to have on the HFT tracking performance. These distortions are the result of an increased space charge in the TPC due to the expected higher luminosities. In answering this question we ignored for the time being the role that the HFT can play in correcting part of those distortions. We made the pessimistic scenario that the only tools available are the ones that STAR is **currently** using to correct existing data. STAR is actively considering upgrades with high resolution calibration chambers that will monitor space charge effects continuously during data taking. A study was performed and the result indicates that, after correcting for the increased systematics, we will be left with a residual error of about 2% of the overall effect ( $\sim 1$  cm effective transverse shift at inner padrow). This translates into an increase of the TPC track projection errors to SSD by  $\sqrt{2}$ . Details about the study that led to the Fast-MC results shown below can be found in the following link<sup>1</sup>.

<sup>1</sup> <http://drupal.star.bnl.gov/STAR/subsys/hft/documents/hand-calculations-j-thomas>





Single Track Efficiency for the HFT (D0 Efficiency dashed) .vs. Pt

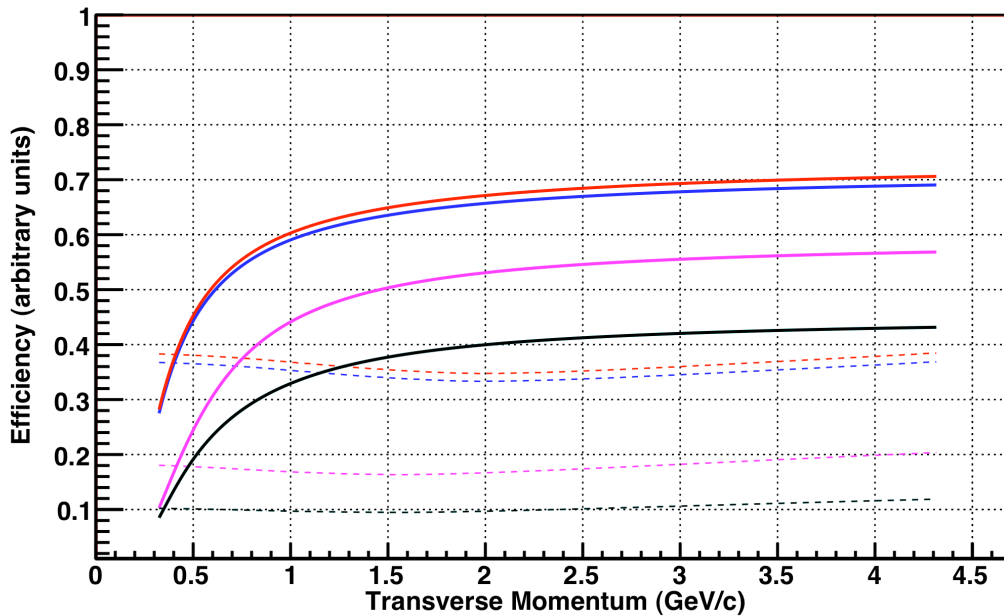


Figure 15: Impact of TPC systematics (space charge) on single track efficiency. See text for explanation of colored lines.

Figure 15 shows the results of a full (upper) and Fast-MC (lower) on the impact of the effect. In the case of Fast-MC the red (normal) and blue lines (increased errors) are ones of primary concern. Both simulations show a minimal impact on system tracking performance. This means that the hit density at the SSD is low enough so that the impact

of a projection error increase by  $\sim 40\%$  is not altering the efficiency of the tracker. The red and blue dashed lines show the impact on the D-meson efficiency before cuts (about 2%). In the same figure the Fast-MC performs the same exercise in the case of both the SSD and IST being inactive in the system. The purple and the black line show the effect of the TPC systematics on such a system. We see that the loss of efficiency almost doubles since the TPC distorted tracks have now to be extrapolated and associated with the PIXEL layer-2 hits that also contain pile-up hits. The purple and dashed lines show the impact on D0 efficiency before cuts. The effect in this case of NoIST and NoSSD is dramatic and catastrophic. We cannot afford to lose both layers of the intermediate tracking system.


## 4. Risk Analysis

### 4.1. Integration Time

**The proposed PIXEL detector is a challenging device. It is dependent on the successful development of high readout speed, and shorter integration time (100-200  $\mu\text{s}$ ) MAPS devices by IRES Strasbourg with good yield.**

MAPS devices have been developed by the IRES group in Strasbourg in a very modular and gradual way pushing the limits of the technology. The exact steps in a long chain of gradual improvements and thorough testing have been described in the HFT proposal.<sup>2</sup> Currently, we are testing a production quantity run of the “Phase 1” sensor. Phase 1 sensors will be used in the prototype engineering run planned for RHIC Run 11 and represent the last step before the “Ultimate” sensor that will be used for the final version of the Pixel detector. The read-out of Phase 1 sensors differs from the Ultimate read-out in as far as for Phase 1 all channels are read out and that zero suppression is done off the sensor chip. This limits the integration time of Phase 1 to 640  $\mu\text{s}$ . The Ultimate technology performs zero suppression in the sensor chip and only transfers the addresses of pixels with a valid hit to the outside world. This on-chip readout results in an integration time of 200  $\mu\text{s}$ , the integration time specified for the HFT. The Ultimate read-out technology has been implemented in test runs with small numbers of pixels and has been tested successfully. What remains to be done is to implement this design for a full size sensor and to finalize the control aspects of the full size chips.

The final design of Ultimate is on the critical path for the Pixel part of the HFT. A delay in finalizing the design and going into production will result in a delay in schedule. A schedule delay will not transform into a cost increase since the IST and the production of the inner support structure do not depend on the readiness of the Pixel detector. The Pixel can be installed independently in a one-day interval.

**The risk for a schedule delay due to not meeting the integration time requirements is low.** The development of the Ultimate is on schedule and there are no known or anticipated showstoppers. 

---

<sup>2</sup> C. Chasman et al., LBNL # 5509-2008,  
[http://rnc.lbl.gov/hft/docs/hft\\_final\\_submission\\_version.pdf](http://rnc.lbl.gov/hft/docs/hft_final_submission_version.pdf)

The schedule risk has been mitigated by a systematic and step-wise approach to sensor development by the IRES group. Also the development and the testing of prototype sensors is performed in close collaboration with the LBNL group. We have instituted a scheme of regular phone discussions and quarterly meetings at Strasbourg where all aspects of the design process and of testing are reviewed, discussed, and coordinated.

## 4.2. Low mass support

**The construction of a low mass support structure, which incorporates power distribution, system cooling and cabling. Further detailed physics simulations are required to understand the optimization of the thin and fragile MAP sensors and the impact of services (e.g. power, readout, cooling) which could dominate the overall material budget of the HFT tracker.**

Our original simulations were carried out using a radiation length of 0.28% for the first pixel layer and a radiation length of 0.14% for the beam pipe. Here we address the physics risk due to increases in the radiation length. The important parameter to be examined is the impact parameter of the pixel detector. The impact parameter resolution (accuracy of pointing to the vertex) can be expressed in the following form:

$$\Delta v = \Delta x \cdot \sqrt{\frac{r_2^2 - r_1^2}{(r_1 + r_2)^2}} \oplus \theta_m \cdot r_1$$

Where  $\Delta x$  is the detector position resolution,  $r_1$  is the inner layer radius and  $r_2$  is the outer layer radius and  $\theta_m$  is the multiple coulomb scattering angle. The second term, the projection error due to the multiple coulomb scattering, is the parameter of interest and it is this term that dominates the detector performance. The multiple coulomb scattering angle is given as:

$$\theta_m = \frac{13.6 \text{ MeV}}{\beta \cdot c \cdot p} \sqrt{X_0}$$

Where  $X_0$  is the fraction radiation length.  $X_0$  is the radiation length for both the inner pixel layer and the beam pipe. In this approximation the beam pipe is assumed to be at the same radius as the inner pixel detector. The original vertex projection resolution which has been used for our simulations is:

$$\Delta v = 13 \mu\text{m} \oplus \frac{22 \text{ GeV}}{p \cdot c} \mu\text{m}$$

As the design of the ladder has matured the radiation length of the ladder has increased from 0.28% to 0.37%. This increase is the result of adding another carbon composite

backing layer plus additional adhesive. This was necessary to maintain sufficient position stability (position stability affects the first term of the pointing resolution expression). The current ladder design has been extensively analyzed for position stability, so further design changes are not expected to be required to meet the stability requirements. The greatest risk to increased ladder radiation length is the aluminum kapton cable. We have a vendor that should be able to produce an aluminum kapton cable, but aluminum kapton has traditionally been difficult, so there is the risk that we might have to use copper in place of the aluminum. If this is required the radiation length of the ladder will increase from 0.37% to 0.51%.

There was also an increase in the beam pipe thickness. Brush Wellman was originally comfortable building a 0.5 mm Beryllium beam pipe, but they have subsequently argued that 0.8 mm would be much less risky and less expensive. The degradations in the impact parameter resolution resulting from these various changes are summarized in Table 1. The last entry in the table is for a copper ladder cable. This is the worst case and results in a pointing resolution that is 32% worse than the original design which was simulated.

Configuration	Beam pipe $X_0$	Ladder $X_0$	Impact parameter resolution, MCS term	% resolution degradation over original
original	0.14%	0.28%	22 GeV· $\mu$ m/p·c	
current with aluminum	0.23%	0.37%	26 GeV· $\mu$ m/p·c	19%
current with copper	0.23%	0.51%	29 GeV· $\mu$ m/p·c	32%

*Table 1: . Summary of radiation length and impact parameter resolution. The original HFT PIXEL design is compared with the current ladder design and the worst case example where the aluminum in the ladder cable is replaced with copper.*

It should be noted that even with these increases the worst case ladder radiation length is still less than 1/2 that of pixel detectors in ATLAS, ALICE or PHENIX.

Simulations (see fig. 15) show that increasing the radiation length of the first pixel layer from 0.32% to 0.62% reduces the significance factor by a factor of 2 in the  $p_t$  region around 0.5 GeV/c. Note this set of values are slightly different from the values discussed above ( 37% and 51%) but in the same general range.

The reduction in significance results in an increased data sample to achieve the same statistical uncertainty as specified in the following expression.

$$N = \frac{1}{U^2} \left( \frac{1}{s} + \frac{b}{s^2} \right)$$

N is the number of events required to achieve a signal measurement uncertainty U.

s is the mean signal per event and b is the mean combinatoric background per event in the peak measuring widow.

This mean that a factor of 4 increase in data is required for  $p_T$  less than 1.5 GeV/c to achieve the same statistical significance and to make up for the 30% increase in the radiation length of the first pixel layer. We can expect some improvement in this increase by optimizing the cuts. The proposal statistics is based on 500M events. It is unlikely that this can be increased by a large factor, unless reconstruction efficiency and projected computing capacity will be larger than currently projected. Design improvements in the ladder flex pc cable are being studied which could result in fewer layers. This could restore the ladder radiation length to 0.3% while still using copper conductors.

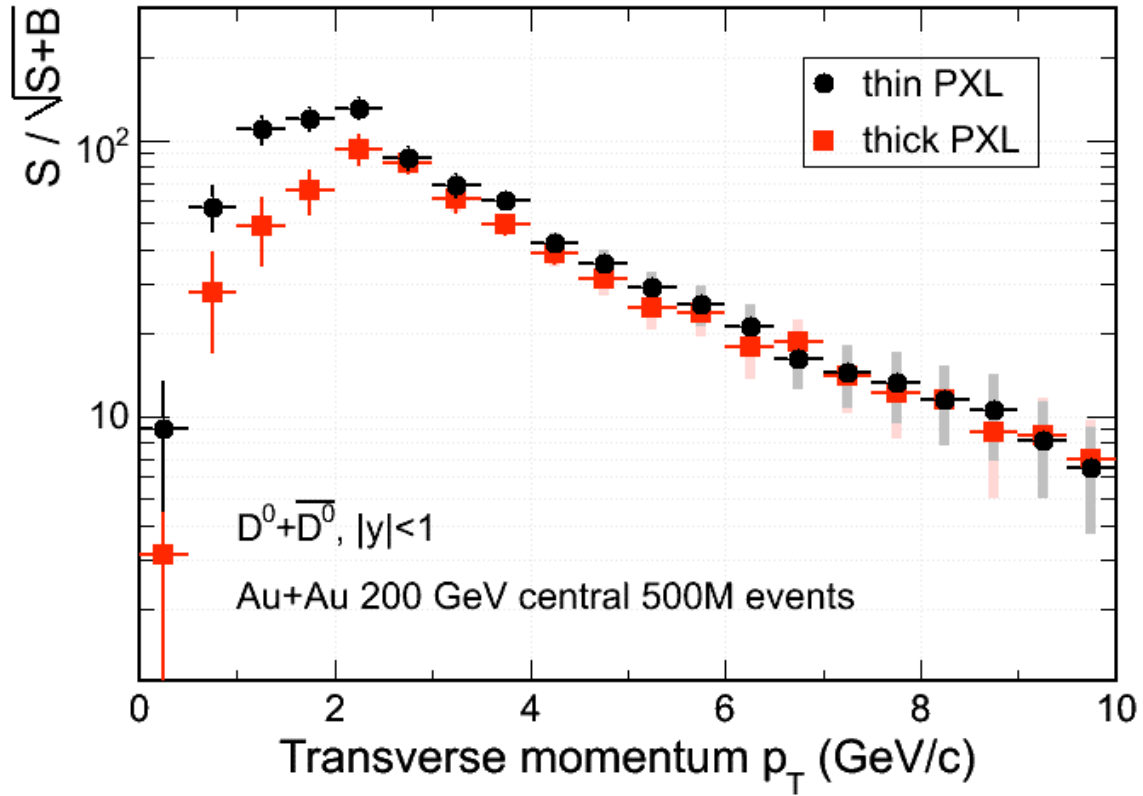


Figure 16: A measure of the significance factor from simulation for a first PIXEL layer with a radiation length of 0.32% and 0.62%. [WHAT ARE THE GREY BANDS?]

### 4.3. Radiation Tolerance

Radiation tolerance of the MAPS devices needs to be carefully studied. This could become an issue in proton running where radiation doses may be well above those considered in the HFT proposal. The reviewers' assessment of the radiation hazard was hindered by the absence of scientific information regarding the utility of the HFT in the 500 GeV spin program. Given the wide range of running conditions expected at RHIC-II, establishing the radiation exposure and the performance degradation of the PIXEL device is a high priority issue that must be addressed.

**This includes the disposition of the PIXEL being easily removable and replaced. The commissioning of a new set of MAP sensors annually struck some reviewers as a challenging prospect.**

We have been studying the radiation environment in the interior of the STAR detector. During Run 8, we installed TLDs on a string between the FTPC and the east BBC. In addition, TLDs were installed on the BBCs. TLDs integrate the total radiation dose over a run including beam tuning.

We used separate TLDs for the d-Au and the p-p run at 200 GeV/c. These results show that the radiation exposure is essentially flat along the beam direction near the BBCs. Using the BBC TLD data we can extrapolate to p+p running at 500 GeV/c at the expected RHIC II luminosity. For a 10 week p+p run at 500 GeV/c the results shown in the table below:


Radius cm			Extrapolated Dose AuAu kRad	Extrapolated Dose – pp 500 kRad
2.5	1/r <sup>2</sup> projection from 5.1 cm	Radius of inner Pixel Detector	34	380
5.1	Extrapolated from a measured point at the BBC		8.2	91
8	Extrapolated from a measured point at the BBC	Radius of the outer pixel layer	4(?)	(40)

There are large uncertainties in this estimate. Therefore, we are repeating these measurements in Run 9 where for the first time we have 500 GeV data. We will separately identify the contributions from ionizing and neutrons by using three sets of detectors. There is a group of TLDs and neutron detectors along the beam pipe on a string. There are neutron and TLD detectors in three circular rows on the East and West BBCs. These items will be measured separately for the 200 GeV and 500 GeV p+p run.

From the present extrapolations, it is obvious that the radiation dose in a 500 GeV p+p run is such that the likelihood for radiation damage during a RHIC run is high for the inner Pixel layer. Given the fact that the Pixel detector does not contribute to the 500 GeV high luminosity spin program, we anticipate the normal running mode to be without the Pixel detector. For the measurement of the charm cross section at 500 GeV we plan to have a dedicated run at relatively low luminosity.

From our current knowledge of the radiation field in STAR and from the measurement of the impact of radiation on detector performance we estimate that for heavy ion running at highest RHIC luminosity the performance of the inner Pixel layer will not deteriorate during one RHIC running year to a degree that it will influence the physics performance of the HFT. The measurements underway will be evaluated in time for the CDR.

Until more detailed knowledge on radiation fields and radiation tolerance we assume that we will have to replace the inner Pixel layer on a yearly basis. Easy replacement is

designed into the Pixel ladders. One should keep in mind that the inner layers represent only one quarter of the active Pixel surface. We plan to produce enough sensors initially to instrument **four copies of the Pixel detector**. 

We have taken several steps to mitigate the risk of radiation damage:

- We are putting a program in place to carefully measure the radiation field at STAR. This will improve our current (projected) estimates of the dose received.
- We have reduced the pixel size to the smallest allowed by our design in the AMS 0.35 technology for our final version of the sensor to enhance the tolerance to radiation damage.
- The Pixel detector is designed to be replaceable within a 24 hour timeframe. Replacement of a detector due to sensor damage is a feature and we will have a total of 4 physical Pixel detectors.
- We are currently investigating (with IPHC) different technologies. Graded doping and high resistivity substrate wafers offer the promise of significantly improved collection times and enhanced radiation protection. The results would be available on a timescale to be useful for the final sensor. In addition, IPHC has an active program improving their amplifier designs to be more radiation tolerant. Mimosas-22 is expected to reach a tolerance of 1Mrad in the next iteration.

#### 4.4.Pile Up

**Event pile-up and beam bunch resolution in proton running could be an issue. Some reviewers were not persuaded by the statement that the RHIC spin program would be able to handle multiple interactions within the same beam crossing.**

The expected interaction rate for the projected RHIC pp luminosity is 12 MHz at 500 GeV and 5 MHz at 200 GeV. This implies an average # collisions per bunch crossing of 1.25 and 0.5 for 500 and 200 GeV, respectively. The primary pp physics goal that utilizes the HFT is a long 200 GeV run for getting reference spectra, envisioned for the second year of running following completion of the HFT. Again we like to stress that due to the expected radiation levels for 500 GeV full luminosity running the pixel layers will not be in situ under those conditions.

The question raised is of concern, but the following analysis shows that the associated risk is small in our opinion. It should be pointed out that this is a general issue for STAR and not related to the HFT inner detector system.

At a rate of 0.5 interaction per bunch crossing (every 107 nsec) of events which has interaction ~23% of these will have 2 or more interactions (assuming Poisson distribution). Due to the distributed vertex ( $\sigma_z \sim 45$  cm) the probability that the vertices for multiple interactions are within a few mm is rather small. The fast detector system in STAR (SSD, IST, ToF, VPD,..) are all used to assist in associating reconstructed track to the respective correctly assigned vertex. This procedure (have been /is) developed in order to deal with data from ongoing high luminosity pp running, in particular from the just completed 500 GeV commissioning run which had interaction rate of up to 3 MHz comparable to the maximum anticipated rate for 200 GeV running. This particular method could have problems for the W-program where the number of tracks in events of



interest is low, but for events with charmed mesons (at 200 GeV) this should be fine.

#### **4.5.IST Design**

**The IST design is considerably less developed than the PIXEL detector. The proponents need to develop a better understanding of support and cooling issues. In particular they need to understand the physics and technical tradeoffs associated with a possible choice of liquid cooling, which will increase the mass of the IST layer. The impact of additional mass on the performance of the tracker, particularly at low momentum should be simulated.**

The design of the IST ladders has greatly advanced since the CD-0 review. The current design calls for room temperature liquid cooling and uses carbon fiber ladders that have been prototyped already. Thus the radiation length of the design is known relatively well. The expected changes before CD-1 will be optimizing iterations with respect to cooling channel dimensions and the accompanying changes in the ladder dimensions. Both the full and fast simulations use the most recent geometry and thus have a realistic material distribution for the IST.

We have performed full simulations where the IST inactive material is doubled from 1%  $X_0$  to 2%  $X_0$  to gauge the effect of unexpected material increase. An IST material budget over 2%  $X_0$  is not acceptable since the resulting conversions would adversely affect the overall performance of STAR. Current design is within this limit, but awaits a final evaluation. As described in Section Full System Performance for various Thickness Scenarios doubling the IST inactive material has minimal impact on the HFT physics even down to low Pt.

The fast simulations show that the addition of liquid cooling only leads to an about 1% loss of single track efficiency in the HFT, even with two rather large cooling channels embedded in the ladders. It is expected that the size of the cooling channels can be reduced and that also the rest of the ladder design can be slimmed down still. The current design can as such be taken as a worst case scenario with a material budget of 1.35%  $X_0$  per ladder.

#### **4.6.Redundancy**

**The HFT performance relies on achieving graded pointing resolution and high efficiency starting from the outside (TPC) and tracking inward towards the PIXEL. The design has little redundancy in tracking layers and thus all three detectors (SSD+IST+PIXEL) must individually perform at high efficiency. The operations and efficiency of the existing detector, SSD, is an ongoing concern from a previous technical review.**

The system of graded pointing resolution has redundancy built in since IST and SSD have similar functions. We have performed physics simulations for the extreme case that either the SSD or the IST fail completely. As described in Section 3.2 the efficiency for D0 is reduced by ~20% if either the SSD or the IST fails completely. In both cases the HFT physics program could proceed.



The existing SSD detector has been disassembled and all ladders tested and repaired. We have 21 fully functioning ladders. This is enough to rebuild the SSD and leaves us with one spare ladder.

We attempt to mitigate the risk posed by the low number of spare ladders. Since we need to reconstruct the suspension of the SSD we are no longer bound to the original SSD ladder configuration and radius. We have started a program of optimizing the SSD and IST geometry with special emphasis on reducing the SSD radius so that additional spare ladders could be gained.

## 5. Appendix

### CD-0 Report Excerpts

2) “The STAR collaboration should perform refined simulations for the HFT that include realistic detector response, particle ID, and TPC space charge effects. These simulations should include extraction of the proposed measurements, such as the  $v_2$ ,  $R_{AA}$ ,  $R_{cp}$  distributions, and  $p_T$  spectra of D mesons embedded in the generated events, and examine the sensitivity of measurements to detector thicknesses. A report articulating the results of these simulations should be submitted to DOE by April 30, 2009, including any influence of the simulation results on the proposed technical performance specifications.”

3) “The HFT collaboration should specifically address the impact on the proposed science inherent in the six risk factors identified at this review, including a failure analysis of each detector layer and submit, by April 30, 2009, a report to DOE articulating its findings.” The six risk factors are identified as follows:

1. The proposed PIXEL detector is a challenging device. It is dependent on the successful development of high readout speed, and shorter integration time (100-200  $\mu$ s) MAPS devices by IRES Strasbourg with good yield
2. The construction of a low mass support structure which incorporates power distribution, system cooling and cabling. Further detailed physics simulations are required to understand the optimization of the thin and fragile MAP sensors and the impact of services (e.g. power, readout, cooling) which could dominate the overall material budget of the HFT tracker.
3. Radiation tolerance of the MAPS devices needs to be carefully studied. This could become an issue in proton running where radiation doses may be well above those considered in the HFT proposal. The reviewers’ assessment of the radiation hazard was hindered by the absence of scientific information

regarding the utility of the HFT in the 500 GeV spin program. Given the wide range of running conditions expected at RHIC-II, establishing the radiation exposure and the performance degradation of the PIXEL device is a high priority issue that must be addressed. This includes the disposition of the PIXEL being easily removable and replaced. The commissioning of a new set of MAP sensors annually struck some reviewers as a challenging prospect.

4. Event pile-up and beam bunch resolution in proton running could be an issue. Some reviewers were not persuaded by the statement that the RHIC spin program would be able to handle multiple interactions within the same beam crossing.
5. The IST design is considerably less developed than the PIXEL detector. The proponents need to develop a better understanding of support and cooling issues. In particular they need to understand the physics and technical tradeoffs associated with a possible choice of liquid cooling, which will increase the mass of the IST layer. The impact of additional mass on the performance of the tracker, particularly at low momentum should be simulated.
6. The HFT performance relies on achieving graded pointing resolution and high efficiency starting from the outside (TPC) and tracking inward towards the PIXEL. The design has little redundancy in tracking layers and thus all three detectors (SSD+IST+PIXEL) must individually perform at high efficiency. The operations and efficiency of the existing detector, SSD, is an ongoing concern from a previous technical review.